

† . * . **

Matching inviscid and boundary layer method for incompressible and compressible flows

Changhyun Sohn, Suyeon Moon and Jeongyun Lee

Key Words: Hypersonic flow(), thick boundary layer()

Abstract

Matching inviscid and boundary layer methods are developed for hypersonic flow with thick boundary layer. The new equations match all the boundary layer properties with a variation in the inviscid solution near the edge, except for the normal velocity. Computational comparison are performed for incompressible and compressible flows over a flat plate. Results from the present method are compared with Navier-Stokes solutions. The present results are in good agreement with Navier-Stokes solutions. They show that the new technique can provide improved heating rates and skin friction predictions for preliminary design of vehicles where shear layers and entropy layer swallowing are important.

1. Introduction

The Navier-Stokes equations [1], although they most accurately describe the fluid flow, require large computer resources and manhours. While Navier-Stokes computations are generally found to be too expensive for design tasks, recently some investigations have been made using classical boundary layer codes. Wuthrich, et. al. [2] have developed coupled Euler/boundary layer method. They used the second-order boundary layer equations. For high Reynolds number, the boundary layer is sufficiently small compared to the shock

layer. One can consider separate calculations for the inviscid shock layer and the viscous boundary layer. Unfortunately, for many hypersonic flows it is not possible to account correctly for the edge conditions within the context of the classical boundary layer method.

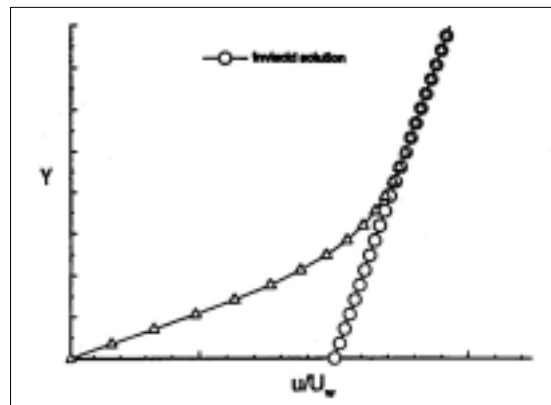


Fig. 1 Velocity profiles for new methods

†
E-mail : chsohn@knu.ac.kr
TEL : (053)950-5570 FAX : (053)950-6550
*
**

Using the classical boundary layer theory established by Prandtl, the variables at the edge of the boundary layer are matched with the inviscid variables at the wall. This is valid for high Reynolds number and significantly thin boundary layers. In hypersonic flows, the Reynolds number is often moderate due to the low density of the gas. In addition, boundary layer thickness becomes no longer negligible compared to the entropy layer thickness. The entropy layer may even be completely 'swallowed' by the boundary layer on the rear part of the body. In such a case, a correct matching cannot be obtained between the inviscid flow and the boundary layer. For that reason Van Dyke[3] proposed utilization of a matched asymptotic expansion which formally derived matching relationships between the viscous and inviscid solutions. The method provided good results, but could only be used for flows whose inviscid solution could be represented with a Taylor Series approximation and would not be valid for hypersonic flows with thick boundary layer. The present method using matching inviscid/boundary layer, however, is correct matching between viscous and inviscid solutions as shown in Fig. 1.

A new defect formulation in the viscous region by Aupoix, et. al.[4] is used with a matched asymptotic expansions technique. For incompressible flows over a flat plate the method under-predicts skin friction and poorly predicts velocity profiles in some cases. For compressible flows, the method predicts better velocity profiles, but underestimates both wall heating and skin friction.

In comparison, the present method presented in this body of work is not limited to inviscid velocities predicted through expansions, but instead uses the data directly from an inviscid finite difference solution.

2. Basic equation

The inviscid equations are

$$\frac{\partial U}{\partial x} + \frac{\partial V}{\partial y} = 0 \tag{1}$$

$$U \frac{\partial U}{\partial x} + V \frac{\partial U}{\partial y} = - \frac{1}{\rho} \frac{\partial P}{\partial x} \tag{2}$$

The laminar boundary layer equations are

$$\frac{\partial u}{\partial x} + \frac{\partial v}{\partial y} = 0 \tag{3}$$

$$u \frac{\partial u}{\partial x} + v \frac{\partial u}{\partial y} - \nu \frac{\partial^2 u}{\partial y^2} = - \frac{1}{\rho} \frac{\partial P}{\partial x} \tag{4}$$

From inviscid continuity equation (1)

$$\bar{V} = \bar{V}_w(x) - \int_0^y \frac{\partial U}{\partial x} dy \tag{5}$$

DeJarnette, et. al. [5] introduced the inviscid transpiration velocity at the wall. $\bar{V}_w(x)$

From boundary layer continuity equation,

$$v(x, y) = - \int_0^y \frac{\partial u}{\partial x} dy \tag{6}$$

Then, the proper matching of the boundary-layer solution with the inviscid solution would have $u=U(x, y)$ and $v=V(x, y)$ for y

$$\bar{V}_w(x) = \frac{d}{dx} \int_0^\delta (U - u) dy \tag{7}$$

Equation (7) gives the transpiration velocity for the inviscid solution.

The basic equation of matching inviscid/boundary layer equation which is introduced by DeJarnette, et. al. [5] is

$$\begin{aligned} u \frac{\partial u}{\partial x} + v \frac{\partial u}{\partial y} - \nu \frac{\partial^2 u}{\partial y^2} \\ = \frac{\partial U}{\partial x} + \bar{V} \frac{\partial U}{\partial y} - \nu \frac{\partial^2 U}{\partial y^2} \end{aligned} \tag{8}$$

3. Compressible boundary layers

The method introduced earlier is applied to compressible, laminar flow over a flat plate or axisymmetric flow. The partial differential equations for a compressible, laminar boundary layer, which express the conservation of mass, momentum, and energy, can be written as follows.

$$\frac{\partial(\rho u r_0^j)}{\partial x} + \frac{\partial(\rho v r_0^j)}{\partial y} = 0 \tag{9}$$

$$\rho u \frac{\partial u}{\partial x} + \rho v \frac{\partial u}{\partial y} - \frac{\partial}{\partial y} \left[(\mu + \epsilon) \frac{\partial u}{\partial y} \right] = - \frac{\partial P}{\partial x} \tag{10}$$

$$\begin{aligned} \rho u \frac{\partial H}{\partial x} + \rho v \frac{\partial H}{\partial y} &= \frac{\partial}{\partial y} \left[\frac{\mu}{Pr} \left(1 + \frac{\epsilon}{\mu} \right) \frac{Pr}{Pr_t} \frac{\partial H}{\partial y} \right] \\ &+ \frac{\partial}{\partial y} \left\{ \mu \left[\left(1 - \frac{1}{Pr} \right) + \frac{\epsilon}{\mu} \left(1 - \frac{1}{Pr_t} \right) \right] u \frac{\partial u}{\partial y} \right\} \end{aligned} \tag{11}$$

The j in equation(9) is equal to 0 for two-dimensional flow and to 1 for axisymmetric flow. In order to remove the singularity at $x=0$ and reduce the growth of the boundary layer in the transformed coordinates as the solution proceeds downstream, most transformations for compressible flows employ the Levy-Lees transformation.[6] The new transformation can be written as follows:

$$\xi(x) = \int_0^x (\rho_e \mu_e U)_w \gamma^2 dx \tag{12}$$

$$\eta(x, y) = \frac{\rho_{ew} U_w \gamma}{\sqrt{2\xi}} \int_0^y \frac{\rho}{\rho_{ew}} dy \tag{13}$$

Define

$$u/U_e = F(\xi, \eta) \tag{14}$$

$$U/U_w = F_e(\xi, \eta) \tag{15}$$

$$f = \int_0^\eta F d\eta \tag{16}$$

$$f_e = \int_0^\eta \frac{\rho_e F_e}{\rho} d\eta + f_{ew} \tag{17}$$

Based on Eqs.(6-8) and Eqs.(12-17), the x momentum equation, Eq.(11), can be written in the following form

$$\begin{aligned} 2\xi \left[F \left(\frac{F}{U_w} \right) \frac{dU_w}{d\xi} \right] + \frac{\partial F}{\partial \xi} - \frac{\partial f}{\partial \xi} \frac{\partial F}{\partial \eta} - \\ f \frac{\partial F}{\partial \eta} - \frac{\partial}{\partial \eta} \left[\left(\frac{\rho \mu}{\rho_{ew} \mu_{ew}} \right) \left(1 + \frac{\epsilon}{\mu} \right) \frac{\partial F}{\partial \eta} \right] \\ = 2\xi \left[\frac{\rho_e}{\rho} \right] F_e \left(\frac{F_e}{U_w} \right) \frac{dU_w}{d\xi} + \frac{\partial F_e}{\partial \xi} - \frac{\partial f_e}{\partial \xi} \frac{\partial F_e}{\partial \eta} - \\ f_e \frac{\partial F_e}{\partial \eta} - \frac{\partial}{\partial \eta} \left[\left(\frac{\rho \mu_e}{\rho_{ew} \mu_{ew}} \right) \left(1 + \frac{\epsilon_e}{\mu_e} \right) \frac{\partial F_e}{\partial \eta} \right] \end{aligned} \tag{18}$$

Define

$$g(\xi, \eta) = \frac{H}{H_{ew}} \tag{19}$$

Then the energy equation, Eq.(12), transforms to

$$\begin{aligned} 2\xi \left[F \left(\frac{g}{H_{ew}} \frac{dH_{ew}}{d\xi} + \frac{\partial g}{\partial \xi} \right) - \frac{\partial f}{\partial \xi} \frac{\partial g}{\partial \eta} \right] - f \frac{\partial g}{\partial \eta} \\ - \frac{\partial}{\partial \eta} \left\{ \frac{l^{**}}{Pr} \right\} \frac{\partial g}{\partial \eta} + l \left[\left(1 - \frac{1}{Pr} \right) \right] \\ + \frac{\epsilon}{\mu} \left(1 - \frac{1}{Pr_t} \right) \frac{U_w^2}{H_{ew}} \frac{\partial}{\partial \eta} \left(F \frac{\partial F}{\partial \eta} \right) \\ = 2\xi \left[\frac{\rho_e}{\rho} F_e \left(\frac{g_e}{H_{ew}} \frac{dH_{ew}}{d\xi} + \frac{\partial g_e}{\partial \xi} \right) - \frac{\partial f_e}{\partial \xi} \frac{\partial g_e}{\partial \eta} \right] - f_e \frac{\partial g_e}{\partial \eta} \\ - \frac{\partial}{\partial \eta} \left\{ \frac{l_e^{**}}{Pr_e} \right\} \frac{\partial g_e}{\partial \eta} + l_e \left[\left(1 - \frac{1}{Pr_e} \right) \right] \\ + \frac{\epsilon_e}{\mu_e} \left(1 - \frac{1}{Pr_{et}} \right) \frac{U_w^2}{H_{ew}} \frac{\partial}{\partial \eta} \left(F_e \frac{\partial F_e}{\partial \eta} \right) \end{aligned} \tag{20}$$

where,

$$\begin{aligned} l &= \frac{\rho u}{\rho_{ew} \mu_{ew}} & l^* &= l \left(1 + \frac{\epsilon}{\mu} \right) \\ l^{**} &= l \left(1 + \frac{\epsilon}{\mu} \frac{Pr}{Pr_t} \right) & l_e^* &= l_e \left(1 + \frac{\epsilon_e}{\mu_e} \right) \\ l_e &= \frac{\rho u_e}{\rho_{ew} \mu_{ew}} & l_e^{**} &= l_e \left(1 + \frac{\epsilon_e}{\mu_e} \frac{Pr_e}{Pr_{et}} \right) \end{aligned}$$

The boundary conditions are

$$\begin{aligned} \text{at } \eta = 0, \quad F = 0, \quad f = 0, \quad g = g_w \quad \text{or} \\ \frac{\partial g}{\partial \eta} = 0 \end{aligned} \tag{21}$$

$$\text{at } \eta = \eta_e, \quad F = F_e, \quad g = g_e \quad \text{and} \quad f = f_e$$

4. Results and discussion

Results from the present method are compared with Navier-Stokes and second order defect boundary method[4]. The first case is that of incompressible, inviscid constant shear flow with $Re=106$ given by the equation, $U/U_w = 1 + 60(y/L)$.

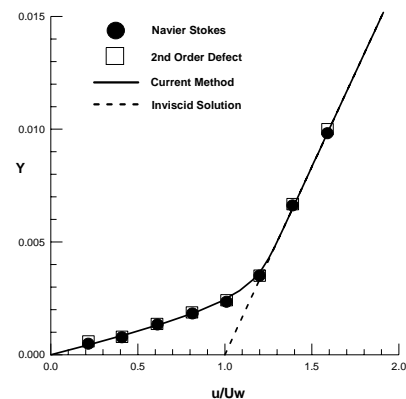


Fig.2 Velocity profiles for constant shear flow at $x/L=0.9$

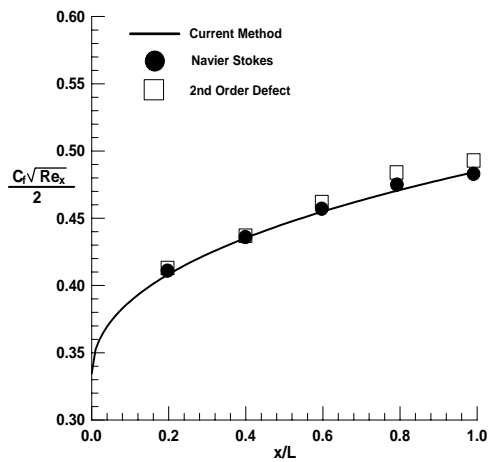


Fig.3 Skin-friction coefficient for constant shear flow

The velocity profile at $x/L=0.9$ is shown in Fig.2 and shows in good agreement with both Navier-Stokes and second order defect boundary method. The evolution of the skin-friction coefficient is plotted in Fig.3. Fig.3 shows a significant increase in the skin-friction coefficient along the flat plate. The traditional first-order boundary layer method gives a constant value of 0.332 that is the same as the present result at the leading edge.

The second case is incompressible inviscid flow with $Re=106$ given by the sinusoidal velocity profile

$$U/U_w = 1 + 0.5 \sin 2[50 (y/L)] \text{ for } y/L \leq 0.01$$

$$U/U_w = 1.5 \text{ for } y/L > 0.01$$

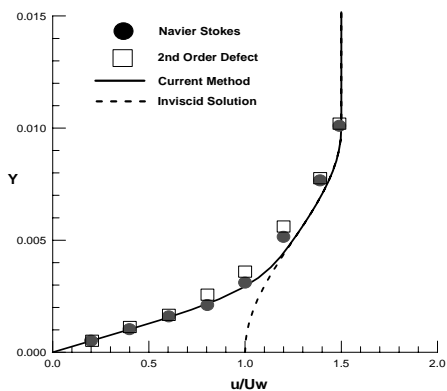


Fig.4 Velocity profiles for sinusoidal shear flow at $x/L=0.9$

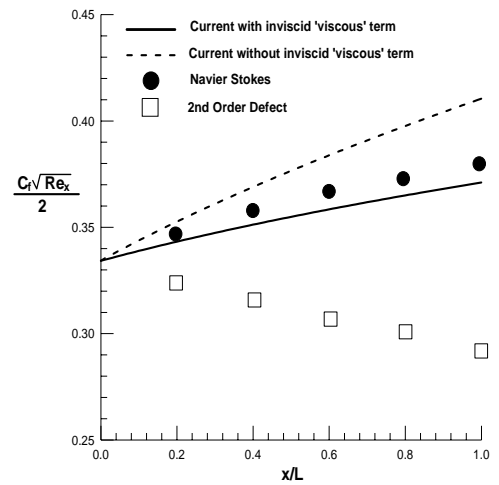


Fig.5 Skin-friction coefficient for sinusoidal shear flow

Velocity profile at $x/L=0.9$ and the evolution of the skin-friction coefficient are shown in Fig.4 and in Fig.5, respectively. They show that the present method agrees well with the Navier-Stokes and second-order defect methods. Aupoix et al.[4] called this case the limit of the boundary-layer approach because their second-order defect method failed to reproduce the N-S skin friction solution as shown in Fig.5. As the velocity profile is poorly predicted in the wall region, the skin friction is underestimated. Fig.5, however, shows that the present method predicts skin friction within 2% of the N-S results. It also shows that the present method with inviscid 'viscous' term, i.e., $(\nu \frac{\partial^2 U}{\partial y^2})$, increases the accuracy of the present method.

The third calculation case is incompressible inviscid shear flow given by the exponential velocity profile

$$U/U_w = \alpha + 1 - \alpha \exp(-\beta y \sqrt{Re}/L)$$

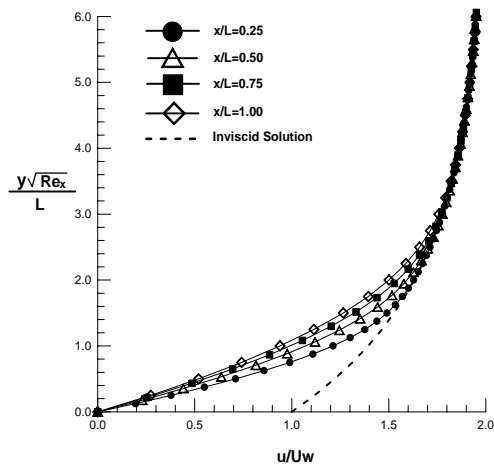


Fig.6 Velocity profiles for exponential shear flow

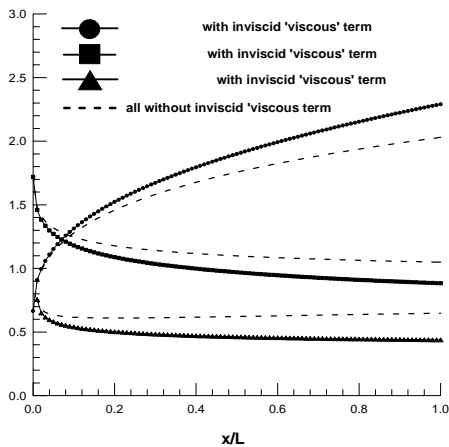


Fig.7 Skin-friction, displacement thickness, and transpiration velocity for exponential shear flow

Results with $\alpha=1$ and $\beta=0.5$ for incompressible flow are shown in Fig.6 and Fig.7. The velocity profiles at five chordwise stations along the plate are shown in Fig.6. At each station, the boundary layer solution merges with the inviscid solution smoothly.

Fig.7 shows the variation of the skin friction, displacement thickness, and transpiration velocity along the surface. Along the plate, the skin friction increases, whereas the displacement thickness and transpiration velocity decrease.

The forth case is compressible shear flow using the exponential inviscid profile given earlier with α

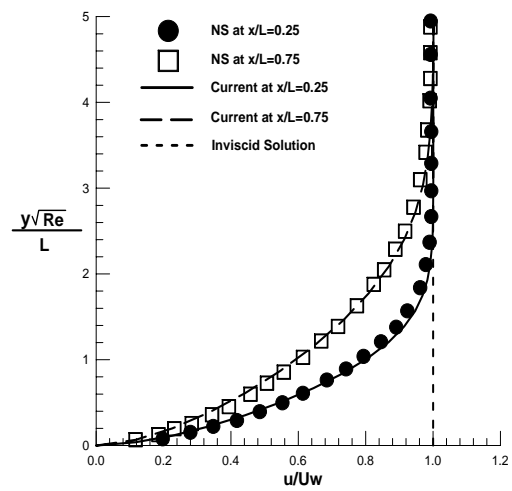


Fig.8 Velocity profiles for cold wall

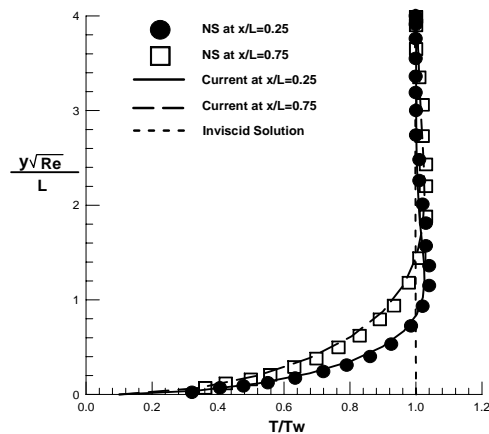


Fig.9 Temperature profiles for cold wall

$=0.1$ and $\beta=0.002$ $Mw=3.$ for a cold wall($T_w/T_e=0.1$)

Fig.8 and Fig.9 compare the velocity and temperature profiles for the cold wall case with Navier-Stokes results[8]. The temperature profiles exhibit the characteristic bump due to viscous dissipation.

Fig.10 and Fig.11 show a nearly uniform distribution of skin friction and heat transfer rate along the plate. Skin friction and heat transfer rate are compare within 4% of the Navier-Stokes results for $x/L \leq 0.2$.

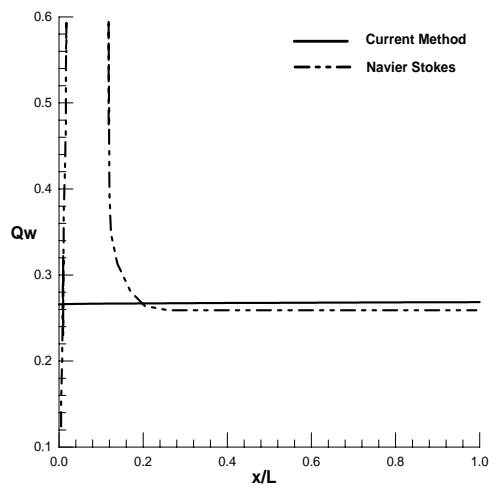


Fig.11 Heat transfer for cold wall

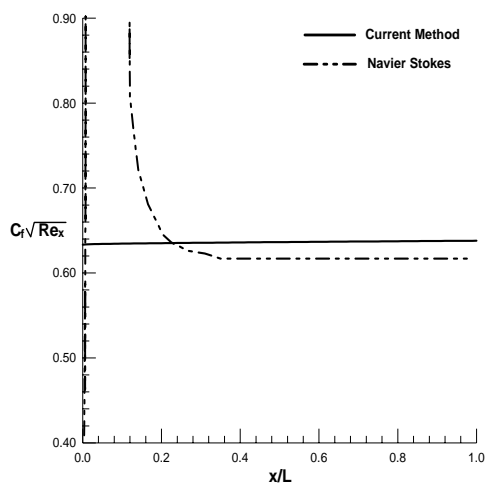


Fig.10 Skin-friction for cold wall

CONCLUSION

Matching inviscid and boundary layer methods are developed for hypersonic flow with thick boundary layer. Results from the present method are compared with Navier-Stokes solutions for various cases, specially entropy layer swallowing is very important flows. The present results are in good agreement with Navier-Stokes solutions. The present method can provide improved heating rate and skin friction predictions for preliminary design of vehicles where shear layers and entropy layer swallowing are important.

REFERENCES

- [1] Anderson, J.D., Hypersonic and High Temperature Gas Dynamics, McGraw-Hill, New York, 1989.
- [2] Wuthrich, S., and Sawley, M. L., "Coupled Euler/Boundary-Layer Method for Nonequilibrium Chemically Reacting Hypersonic Flows," AIAA Journal, Vol.30, No.12, 1992, pp.2836-2844
- [3] Van Dyke, M., "Higher-Order Boundary-Layer Theory," Annual Review of Fluid Mechanics, 1969, pp.265-292.
- [4] Aupoix, B., Brazier, J. P., and Cousteix, J., "Asymptotic Defect Boundary-Layer Theory Applied to Hypersonic Flows," AIAA Journal, Vol.30. No. 5, 1992, pp. 1252-1259.
- [5] DeJarnette, F.R. and Radcliffe, R.A., "Matching Inviscid/Boundary-Layer Flowfields," AIAA Journal, Vol.34. No. 1, January 1996, pp. 35-42.
- [6] Hamilton, H. H., Millman, D.R., and Greedyke, R.B., "Finite-Difference Solution for Laminar or Turbulent Boundary Layer Flow over Axisymmetric Bodies with Ideal Gas, CF₄, or Equilibrium Air Chemistry," NASA TP-3271, 1992
- [7] Harwell, K.E., Matching Boundary-Layer and Inviscid Flowfields at Hypersonic speeds, Ph.D thesis, North Carolina State University, 2000.
- [8] Edwards, J. R., "Development of a Upwind Relaxation Multigrid Method for Computing Three-Dimensional Viscous Internal Flows," AIAA Paper 95-0208, Jan. 1995.
- [9] Coles, Donald: Measurements in the Boundary Layer on a Smooth Flat Plate in Supersonic Flow. Measurements in a Flat-Plate Boundary Layer at the Jet Propulsion Laboratory. Rep. No. 20-71 (Contract No. DA-04-495-Ord 18), Jet Propulsion Lab., California Inst. of Technology, June 1, 1953.